Evaluation of Escherichia coli hydrogenases in persistence

Chandra Shekhar (cs.arya@hotmail.com)
Hokkaido University Graduate School of Information Science and Technology: Hokkaido Daigaku Daigakuin Joho Kagaku Kenkyuka https://orcid.org/0000-0002-0107-0284

Tomonori KAI
Kyushu Institute of Technology Graduate School of Life Science and Systems Engineering: Kyushu Kogyo Daigaku Daigakuin Seimeitai Kogaku Kenkyuka

Thomas K. WOOD
Pennsylvania State University Main Campus: The Pennsylvania State University - University Park Campus

Toshinari MAEDA
Kyushu Institute of Technology Graduate School of Life Science and Systems Engineering: Kyushu Kogyo Daigaku Daigakuin Seimeitai Kogaku Kenkyuka

Research Article

Keywords: Bacterial persistence, Hydrogenases, Escherichia coli, antibiotic stress

Posted Date: March 16th, 2022

DOI: https://doi.org/10.21203/rs.3.rs-1402538/v1

Abstract

Persistence enables a subpopulation of tolerant bacteria to survive in the presence of a bactericidal antibiotic. Reports indicate the non-inherited nature of persistence; however, it also seems to be a genetically influenced phenomenon that has evolved to allow the organisms to survive in sudden environmental insults. In contrary to some reports, lowered available pool of ATP, NAD, and ROS leads to increased survival via slowing down the metabolism and resulting in an increased persister fraction. In this study, the hydrogenases of *Escherichia coli* were analyzed for their role in persistence, where four hydrogenase operon deletion mutants were evaluated before and after antibiotic treatment. As result, the expressions of hydrogenases and cellular viability (specifically hyd-1, 2, 3) were found elevated in antibiotic-treated cells, indicating their influential roles in persistence. Further work elucidated the affected ATP, NAD, and metabolism in the antibiotic-treated mutant cells. The transcriptomic analysis further revealed a wide genomic connectivity of hydrogenases to influence persistence in *E. coli*. Hydrogenases were mainly reported for their essential roles in bacterial hydrogen metabolism, this study further demonstrates their probable role in bacterial survival against antibiotic stress.

Introduction

Persisters are the multidrug-tolerant phenotypic variants of the wild type that have entered a nongrowing dormant state to protect from the lethal action of antibiotics (Wood et al. 2013; Wood 2016). Along with the non-inherited nature of persistence, another view formulates it as a programmed phenomenon with a genetic basis that has evolved to allow the organisms to survive sudden environmental insults (Maisonneuve et al. 2014; Wilmaerts et al. 2019). It has been recently shown that a decrease in adenosine triphosphate (ATP) facilitates the drug tolerance of persisters since most bactericidal antibiotics act by corrupting energy-dependent targets (Shan et al. 2017). Furthermore, the elevated proton motive force (PMF) generated by the oxidation of nicotinamide adenine dinucleotide (NADH) facilitates the uptake of antibiotics that lead to cell death (Allison et al. 2011) through the damages caused by superoxide ions originated by the activities of the antibiotics. (Kohanski et al. 2007). Our hypothesis makes an appearance out of these facts stating that the loss of protein complexes of the membrane, which is supposed to influence energy and metabolism (such as hydrogenases), might have an influential ability on the pool of ATP or NADH, superoxide ions, and therefore survival against antibiotics.

Hydrogenases are enzymes known for their roles in hydrogen metabolism by catalyzing the reversible reaction of hydrogen to protons and electrons (Maeda et al. 2018, Shekhar et al. 2021). The four hydrogenases of *Escherichia coli* (*E. coli)*, abbreviated as, Hyd-1, Hyd-2, Hyd-3, and Hyd-4, are encoded by *hyaABCDEF*, *hybOABCDEFG*, *hycABCDEFGHI*, *hyfABCDEFGHI* operons respectively (Maeda et al. 2018). Hyd-1 is coexpressed with a cytochrome oxidase (Brondsted et al. 1996), which suggests its physiological role is most likely to operate at the anaerobic/aerobic switch. Hyd-2 is popularly known as reversible or bidirectional hydrogenase that can work as a redox pressure release valve to maintain the redox balance of the cell (Pinske et al. 2015). Hyd-2 incorporates hydrogen oxidation to the generation of a transmembrane electrochemical gradient (Pinske et al. 2015). Being a component of the formate

hydrogenlyase (FHL) complex, Hyd-3 connects formate oxidation to proton reduction and is responsible for the majority of sustained hydrogen metabolism in *E. coli* (Bohm et al. 1990). Based on the sequence identity, most of the components of Hyd-3 have equivalents in the respiratory NADH dehydrogenase Complex I (Marreiros et al. 2013). Based on these evolutionary links with Complex I, Hyd-3 activity to the membrane is supposed to be associated with proton translocation and thus energy conservation. In *E. coli* Hyd-3/FHL could be an energy-conserving system (Batista et al. 2013). Hyd-4 is closely related to Hyd-3 and consequently, evolutionarily links to Complex I (Andrews et al. 1997). This report is further supported by the structural arrangement in the membrane domain of Hyd-4, which indicates it's more closely related to Complex I than that of Hyd-3. Hyd-4 is, therefore, is more likely to be coupled in the generation of the transmembrane electrochemical gradient (Marreiros et al. 2013). Genetic analysis suggests that the Hyd-4 may be able to transduce free energy released during the FHL reaction to the generation of a transmembrane ion gradient (Batista et al. 2013). Mycobacterial hydrogenases were found differentially expressed and active during growth and persistence, which suggests that hydrogen oxidation is important for microbial existence in a non-replicative, persistent state (Cordero et al. 2019). For *S. Typhimurium*, the use of molecular hydrogen by uptake hydrogenases is essential for its virulence (Benoit et al. 2019). Moreover, the pathogenic Helicobacter species *H. pylori* and *H. hepaticus* can respire hydrogen through a respiratory [NiFe]-hydrogenase, whereas a mutant hydrogenase strain of *H. pylori* is much less efficient in its colonization in mice (Olson et al. 2002). These reports indicate the pivotal role of hydrogenases in bacterial virulence and viability. Highly purified bidirectional hydrogenase of *Clostridium pasteurianum* could rapidly reduce several 2-, 4- and 5-nitroimidazole compounds via an electron carrier-coupled mechanism, indicating hydrogenase mediated survivability (Church et al. 1990). It was hypothesized before that endogenous or exogenous hydrogen can reduce the killing effect by neutralizing cytotoxic hydroxyl radicals (OH•) since a bactericidal treatment induces bacterial death via OH• (Kohanski et al. 2007). Interestingly, hydrogen selectively could reduce the OH•, the most cytotoxic of reactive oxygen species (ROS), and effectively protected cells, and thus can be used as an effective antioxidant therapy (Ohsawa et al. 2007). A few studies reported that hydrogenases are crucial for bacterial growth inside the gut (Maier et al. 2014; Olson et al. 2002), therefore, hydrogenases or hydrogen metabolism in the bacteria could be assumed to effectively reduce the susceptibility to antibiotics and facilitate antibiotic tolerance to enhance bacterial survival (Nie et al. 2012).

In this study, the four-hydrogenase operon deleted strains of the *E. coli* were employed, and the roles of oxygen, ROS, ATP, NAD, and the key metabolic pathways were elucidated to formulate the significance of hydrogenases in persistence. As a result, hydrogenases (specifically Hyd-2 and Hyd-3) were observed as relatively more influential in the persistence. This work not only provides an understanding of hydrogenases in persistence but also indicates their crucial in the physiology of the bacterial cell.

Materials And Methods

Bacterial strains, media, and growth conditions

E. coli K-12 BW25113 was used as the parent strain (abbreviated as PS) in the study. Each hydrogenase operon mutant investigated in this study was constructed in our previous study (Shekhar et al. 2021) by the one-step inactivation method explained by Datsenko and Wanner (Datsenko et al. 2000). All the strains including operon mutants employed in this study are listed in Table 1. The strains were initially streaked from −70°C glycerol stocks on Luria-Bertani (LB) (Maeda et al. 2007) agar plates, and a single colony was used to inoculate to grow at 37°C for overnight (in the presence of kanamycin, 50 µg/mL, in case of mutants). For the persistence and all related assays, ampicillin (50 µg/mL) was mainly employed to get persister (referred to as 'antibiotic-treated) cells. A fresh culture was prepared in 250 mL flask (Iwaki, Japan) containing 50 mL LB at 37°C with shaking at 180 rpm using a bioshaker (BR-180LF, Taitec). All experiments were conducted using at least three biological replicates. The medium containing 10 g/L Bacto Tryptone, 5 g/L yeast extract, and 5 g/L NaCl was used to grow the strains. The final concentrations of each antibiotic used in LB-ampicillin, LB-chloramphenicol, and LB-kanamycin media or plates were 50 µg/mL ampicillin, 30 µg/mL chloramphenicol, and 50 µg/mL kanamycin, respectively. Carbenicillin (10 µg/mL) was used in place of ampicillin whenever necessary. Chemicals were purchased from Wako Pure Chemical Industries Ltd. (Osaka, Japan), Dojindo Molecular Technologies, Inc. (Kumamoto, Japan), Sigma-Aldrich Co. LLC (Tokyo, Japan), and Nacalai Tesque, Inc. (Kyoto, Japan).

Persister assay

The persister assay was performed as per previous explanations with some modifications (Chowdhury et al. 2016; Wang et al. 2017). Cultures were grown aerobically at 37 °C with shaking at 180 rpm overnight and then diluted (1:1000) in LB medium. The diluted cultures were incubated until cultures reached the mid-exponential phase ($OD_{600nm} \approx 0.8$) aerobically since this phase is characterized to increase the number of persisters more than lag or early exponential phase (Keren et al. 2003; Wang et al. 2017). Cells were then exposed to 50 µg/ml ampicillin, and cultures were incubated for 3 hrs at 37 °C with shaking at 180 rpm. To measure cell viability, samples were taken before and after antibiotic treatment, washed and serially diluted in 0.85% (w/v) NaCl solution, plated on LB agar, and grown overnight at 37°C to determine CFU/mL. Experiments were performed with at least two independent cultures. For convenience in explanation, cell populations before and after antibiotic exposure is termed as 'initial' and 'treated', respectively. The initial cells that were provided full growth, i.e., without the influence of antibiotic, were also included in some experiments for the comparative analysis with treated cells, which are referred to as 'untreated'.

Dissolved-Oxygen Measurements

Dissolved oxygen (DO) levels within culture flasks were determined using a dissolved oxygen sensor of Custom (DO-1000PE) according to the manufacturer's instructions. The 50 ml cultures of initial and treated cell populations were prepared as above and used to monitor DO before and after ampicillin

treatment at different growth levels. The oxygen sensor was calibrated to media at 37 °C. All measurements were obtained from three separate cultures.

Total RNA extraction and quantitative reverse transcription PCR (qRT-PCR)

The initial and treated cell populations were grown as explained above and removed from the cultures to collect the pellets for RNA extraction using 100 µl RNALater solution (Applied Biosystems Foster City, CA) in 2 ml screw-cap tubes after centrifugation at 13000 rpm, 1 min. The tubes containing cell pellets were immersed in 100 ml of dissolved dry ice in ethanol (95%) for 10 s and stored at -70°C before RNA extraction. Total RNA was extracted using a bead beater model 3011b (Wakenyaku Co. Ltd., Japan) and the RNeasy Mini Kit (Qiagen, Inc., Valencia, CA) as explained in (Mustapha et al. 2018). A StepOne Real-Time PCR system and Power SYBR green® RNA-to C_T™ 1- Step kit (Applied Biosystems, Foster City, CA) were used for the transcription analysis of the expression of four hydrogenases in each hydrogenase operon mutant. Housekeeping gene *rrsG* (16S rRNA) was used to normalize the expression data. RNA extracted from the PS was used as the reference template. All the primers used for this transcription analysis are listed in Table 2. Two technical replicates of the samples were performed. The expression of the listed genes was analyzed using 50 ng of total RNA and the collected data was analyzed through relative quantification for qRT-PCR ($2^{-\Delta\Delta CT}$) (Pfaffl et al. 2001).

DNA library preparation and high-throughput sequencing

The DNA library preparation was performed using the Nextera XT DNA Library Prep Kit (Illumina), following the manufacturer's recommended protocol. Briefly, the cDNA was subjected to simultaneous fragmentation and tagmentation to cleave the DNA by Nextera transposome enzyme. The cleaved DNA was subjected to PCR amplification for barcoding the samples with a dual adapter index with a unique barcode sequence (Nextera XT Index kit) to differentiate each sample. Then, the PCR products were purified using Agencourt AMPure XP beads (Beckman Coulter Inc., CA, USA) and normalized using the Nextera XT Library Normalization Beads before pooling all the samples. The normalized and pooled sample was loaded in a 600-cycle V3 MiSeq reagent cartridge kit (Illumina) for sequencing in the Illumina MiSeq sequencer. Sequencing was performed for 301, 8, 8, and 301 cycles for forward, index 1, index 2, and reverse reads, respectively. The raw sequence data has been deposited in the National Center for Biotechnology Information (NCBI) under the Short Reads Archive (SRA) accession number PRJNA671558.

RNA Seq data analysis

FASTQ formatted raw reads were subjected to quality assessment to determine whether the raw reads were qualified for mapping by fastQC (Andrews 2010) and trimmed using cutadapt tool (Martin 2011)

based on the Phred score quality cutoff >=30. The trimmed good quality reads were mapped to the reference genome of *Escherichia coli* str. K-12 substr. MG1655 [NCBI Reference Sequence: NC_000913.3]. The software Rockhopper (McClure et al. 2013) was employed to map on the reference genome, as explained previously (Liu et al. 2020; McClure et al. 2013). Gene expression was normalized by calculating Reads per Kilobase per Million Mapped Reads (RPKM) (Liu et al. 2020). The differential gene expression analysis was done by using the edgeR tool (Robinson et al. 2010), and significant genes were filtered with p-value <=0.05. Upregulated and downregulated genes were filtered with fold change >=0.8 and <=-0.8, respectively. The significantly altered metabolic pathways were obtained through KEGG (Kyoto Encyclopedia of Genes and Genomes) (Kanehisa et al. 2000) and gene ontology (GO) (Young et al. 2010) pathway enrichment analysis with the threshold of p-value < 0.05. The functional annotations were retrieved from UniProt, David, EcoCyc, and NCBI databases. The final normalized data indicating the full list of all differentially expressed genes (DEGs) in initial, treated, and untreated mutant cells are listed in Table S1A-1D, S2A-2D, and S3A-3D respectively.

ATP assay

Intracellular concentrations of ATP in the initial, treated, and untreated cell populations were determined by using a bioluminescent ATP assay kit (FLAA/Sigma), with some modifications from the manufacturer's instructions. Briefly, the pellet was collected from 1mL (8000rpm/2min/4℃) cultures of initial, treated, and untreated strains. The cells were washed twice with pre-chilled PBS (1×) and resuspended in 1mL pre-chilled PBS (1×). The cell resuspension was neutralized (pH ≈7.8) using a 5M NaOH solution followed by cellular lysis by trichloroacetic acid (final concentration 1%). 100µl of ATP Assay Mix solution was added to the wells. Swirled and allowed to stand at room temperature (RT) for ~3 min. Rapidly added 100µl of sample to the reaction wells of 96-well plate. They were swirled briskly to mix and immediately measured the amount of light produced using a luminometer (Thermo Scientific VARIOSKAN FLASH 5250040). Each assay run included a blank sample and ATP standard sample to remove the noise values. All samples were prepared and analyzed in quintuplets.

NAD/NADH assay

NAD and NADH levels, in which NAD represents the sum of NAD^+ and NADH, were measured according to the manufacturer's instructions of the assay kit (Abcam, ab65348). In brief, the pellet was collected from 1mL of initial, treated, and untreated cell cultures by centrifugation at 4000 rpm, 4 °C for 10 min. Cells were washed with ice-cold phosphate buffer solution (PBS) and then extracted with 400µL of NADH/NAD Extraction Buffer by two freeze/ thaw cycles of 20 minutes at − 70 °C followed by 10 minutes at RT. To remove any insoluble material the extraction was centrifuged for 5 minutes, 4°C at top speed after a short vortex of 10 seconds. To measure total NAD (NAD), 50µl of each sample supernatant was mixed with 100µl Reaction Mix (containing NAD cycling buffer and NAD Cycling Enzyme Mix) and incubated at RT for 5 min to convert NAD^+ to NADH, followed by the addition of 10µl NADH developer buffer and 2 h

incubation at RT. To quantify the NADH, NAD^+ from 200µL of each extracted sample was decomposed by incubation at 60 °C for 30 min before measurement. OD_{450nm} values were then read using a microplate reader (Thermo Scientific VARIOSKAN FLASH 5250040).

Reactive oxygen species assay

For the ROS measurements, we used the Molecular Probes™ Carboxy-H_2DCFDA kit (Invitrogen #C400) according to the manufacturer's instructions and previously described (Wang et al. 2017). In brief, the initial, treated, and untreated cell populations were grown at 37°C/180rpm and removed from the cultures as explained above to estimate the ROS levels. The 1mL cultures of each strain were washed twice with pre-warmed PBS (1×) buffer (pH 7.4). After a short incubation at 37°C, the cells were further resuspended in 1 ml 25µM carboxy-H_2DCFDA reconstituted with PBS buffer and incubated for 30 minutes at 37°C, in the dark. 200µl of the supernatant and cells transferred into 96-well plate separately to record fluorescence at 492/525 nm and optical density at 600 nm respectively using a microplate reader (Thermo Scientific VARIOSKAN FLASH 5250040).

Results

To work upon the hypothesis, four hydrogenases operon deletion mutants were exposed to a dose of antibiotic (ampicillin) at their mid-exponential phase. Ampicillin was chosen as it is widely used for persister isolation (Wang et al. 2017; Lewis 2019). The cells before and after antibiotic treatment were evaluated for a certain persistence associated with metabolic phenomenon.

Hydrogenase operon deletion enhanced cell viability:

To evaluate the hydrogenase mediated cell viability during the antibiotic-induced persistence, the colony-forming unit (cfu) of the four hydrogenase mutants was estimated by counting the colonies before and after antibiotic treatment, as follow:

$$Cellular\ viability = \frac{\text{cfu/mL obtained from the antibiotic} - \text{treated culture}}{\text{cfu/mL obtained from the initial cells}}$$

Along with the operon deleted mutants their respective large subunit gene deleted mutants were also included for the comparative analysis and to predict the impact of complete operon deletion over a single gene. As a result, the cellular viability of the mutants was found increased from the antibiotic-treated cultures of all the hydrogenase large subunit gene and operon mutants compared to the PS (Fig. 1A). However, no significant change was observed in the number of viable cells before antibiotic treatment

from all the mutants, the cell viability was found comparatively more in the case of large subunit gene deletion mutants, indicating operon deletions are more deleterious than single-gene deletions, as shown by our previous study (Shekhar et al. 2021). From both types of deletions, *hyb* and *hyc* were noted vital for bacterial survival since the viabilities were 20- and 18-fold increased respectively from the PS.

Along with their viabilities under micro-aerobic (oxygen deprived, explained later) conditions, *hyb* and *hyc* operon deletions were also found significant under strict anaerobic conditions, due to their comparable more cellular viabilities (Fig. 1B). *hya,* and *hyf* deletions also showed slightly increased viability as compared to the PS, although it was lower than *hyb*, *hyc* deletions. Importantly, cellular viabilities were noted reduced under anaerobic conditions than micro-aerobic ones (Fig. 1A and 1B). Additionally, results showed that the influence of the four hydrogenases is not similar indicating their different physiological functioning under similar conditions.

Impact of antibiotic on the growths of the mutants and the role of the dissolved oxygen in hydrogenase-mediated persistence:

Since persister level increases during growth (Keren et al. 2004; Lewis 2019), it is important to evaluate the growth of the strains in the presence and absence of the antibiotic. The growth of each hydrogenase operon mutant was monitored during the persister assay. A control group of the same strains was simultaneously monitored where no antibiotic was supplemented. As result, in the absence of antibiotic, relatively reduced growth of the mutants was observed compared to the PS, specifically, *hyb* and *hyf* mutants (Fig. 2A). Although not significant, a reduction in the growth of each mutant was noted when grown in the presence of antibiotic (data not shown). The growth differences between antibiotic-treated and untreated states of the mutants were minimum in the case of *hyb* mutant compared to other strains (data not shown), which may indicate a relatively more ability of this mutant to grow in presence of antibiotic. As *E. coli* grows, the level of persisters dramatically increases (Keren et al. 2004; Lewis 2019), therefore, *hyb* mutant is supposed to give a greater number of persisters as supported by its high cellular viability (Fig. 1B). However, *hyf* mutant showed similar differences as other strains, indicating despite its lower growth, it might not be significant in persistence, since ampicillin treatment leads to the persisters formation by killing cells that are unable to obtain the persister state or less fit to fight the effects of the antibiotic to enter a state of persistence (Hong et al. 2012).

Furthermore, the concentration of the DO in the cultures was monitored at different time points during the persister assay where all the strains showed rapid consumption of oxygen (Fig. 2B). In a result, the oxygen level found dropped near to zero indicating an oxygen deprived state of the culture (referred to as micro-aerobic state, Shan at al. 2012) at their mid-exponential phase i.e., the point at which antibiotic was added to the culture of each mutant. Oxygen consumption rate observed dissimilar among them, where *hyf* mutant found slower and *hyb* mutant found relatively faster indicating higher oxygen exhaustion rate. As reported, the survival of persisters requires a small (20%) drop in DO saturation, and at high DO

concentration levels, the persister population is killed over time (Grant et al. 2012). The cultural conditions, in this study, before and after antibiotic treatment, representing nearly zero oxygen concentrations, may indicate the presence of that subpopulation that is susceptible to act as a persister population.

Hydrogenase expressions elevated after antibiotic treatment:

The test conditions of cell populations before and after antibiotic treatment were micro-aerobic (oxygen deprived), as confirmed by DO assay (Fig. 2B). Although hydrogenases functions were mostly reported from anaerobic conditions (Maeda et al. 2018; Vardar-Schara et al. 2008; Trchounian et al. 2012), some reports are indicating their activity under aerobic or micro-aerobic conditions also (Olson et al. 2002; Cordero et al. 2019). Therefore, this was interesting to evaluate the expression of hydrogenases in the absence and the presence of the antibiotic. In this regard, the expression of the gene encoding the large subunit of each hydrogenase was evaluated from each hydrogenase operon mutant. As a result, as expected, the expression of hydrogenases was found very low in the cultures of initial cells (indicated with '- ') (Fig. 3). Previously, the expression of Hyd-1 and Hyd-2 was found to be maximum under anaerobic conditions (Richard et al. 1999; Maeda et al. 2018); Hyd-3, repressed by oxygen (Pecher, 1983); and Hyd-4, normally do not transcribe or shows very low transcription (Trchounian et al. 2012). These reports support the lower or almost no expression obtained, in this study.

Interestingly, hydrogenase expression was found elevated in the antibiotic-treated (indicated with '+ ') mutant cells (specifically *hya, hyb,* and *hyc*) (Fig. 3). Antibiotic treated *hya* mutant cells showed relatively higher levels of hydrogenase expressions than other strains, however, *hyf* mutant did not show any change in the expression of hydrogenases before and after antibiotic treatment. These elevated hydrogenase expressions under the influence of antibiotic may indicate a significant association of hydrogenases with persistence.

Altered ATP levels after antibiotic treatment:

It was commonly observed that the formation of persister cells is inversely correlated with metabolic activity and energy production (Lewis 2019). ATP was found as a general cause of tolerance since most bactericidal antibiotics kill by corrupting active, energy-dependent targets (Shan et al. 2017). Moreover, variation in the level of ATP served as a mechanism of persister formation in *E. coli* (Lewis 2019; Shan et al. 2017). Therefore, quantification of ATP was realized important, and initial, treated, and untreated cells were evaluated. As a result, the treated cells were found to have a reduced amount of ATP as compared to their untreated state (Fig. 4). The percentage decreased ATP (from untreated to treated) was found maximum in *hyb* and *hyc* mutants (31% and 27% respectively), whereas it was comparatively less in the

case of *hya* and *hyf* (21% and 18%), also in the PS (18%). The relatively lower level of ATP in *hyb* mutant may indicate its more significance in persistence.

Altered levels of total NAD in the antibiotic-treated cells:

As reported, low metabolic activity is the key to the survival of persister cells, since in exponentially growing cultures, persisters were found significantly more abundant in the least redox-active subpopulation (Wood et al. 2013; Mehmet et al. 2015). To elucidate the role of hydrogenase operon deletions and their influence on the total NAD content of the cell, total NAD (NAD^+ and NADH) and NADH were quantified from the cultures of the strains. As a result, the NAD/NADH ratios were estimated reduced in all antibiotic-treated mutant cells (Fig. 5). Although, *hyb* mutant with a relatively more and *hyc* mutant a less NAD/NADH ratio indicating their lowest and highest fold change decrease than other mutants, respectively, these results may indicate a weakened metabolism of all the antibiotic-treated strains. In support of that, the KEGG pathway enrichment analysis also showed a similar result when metabolically important pathways were considered (Fig. 6, Table S4A-4D). All the treated mutants showed reduced amino acid biosynthesis and degradation, carbohydrate biosynthesis and degradation, cell wall biogenesis, energy metabolism, glycolysis, lipid metabolism, metabolic intermediate biosynthesis, oxidative phosphorylation, and TCA cycle compared to their respective untreated ones. *hyc* operon mutant showed relatively more reduced metabolism than *hyb* operon mutant in its treated state than untreated. The reduced metabolism of the strains may indicate its facilitation to the persistence and thereby significant cellular viabilities (Fig. 1A).

Altered ROS levels in the antibiotic-treated strains:

Recent studies have suggested that ROS can provide a protective effect against the antibiotics by inducing persistence as well as contributing lethality to the antibiotics to kill them (Dwyer et al. 2014; Brynildsen et al. 2013; Kohanski et al. 2010). The ability of ROS to both protect and kill bacterial cells motivated us to quantify it in all the strains. As result, the ROS quantity which was detected relatively the same in all the strains before antibiotic treatment found significantly altered after antibiotic treatment, except *hyb* mutant (Fig. 7). In comparison with the untreated cells, antibiotic treatment demonstrated ROS surge in the strains.

As bacterial survival against antibiotic is mediated by the ability to detoxify ROS (Grant et al. 2012; Lewis 2019), the significantly decreased ROS in treated *hyb* mutant cells may be indicating its ability to detoxify or scavenge the ROS induced by the action of the antibiotic. This further justifies the high cellular viability of *hyb* mutant after antibiotic treatment. Contrary to *hyb*, the increased ROS levels in *hya*, *hyc*, and *hyf* operon mutant may reflect their association to the ROS-mediated protective effects against antibiotics (Dwyer et al. 2014; Brynildsen et al. 2013).

Gene ontology (GO) enrichment analyses of hydrogenase-mediated persistence:

To understand further the influential role of hydrogenases in persistence, the change in global gene expression in the antibiotic-treated mutant cells was investigated through transcriptomics analysis (Table S5A-5D). The influenced biological process (BP), cellular component (CC), and molecular function (MF) were identified using the GO enrichment analysis approach (Young et al. 2010). The top 20 GO terms ranked based on most upregulated in treated samples are presented through plots (Fig. S1-S4). In results, the translation, large ribosomal subunit, cellular response to DNA damage stimulus, carbohydrate metabolic process, protein folding and transport, cell division and cycle, response to the antibiotic, tricarboxylic acid cycle, and phosphoenol pyruvate-dependent sugar phosphotransferase system were found most commonly altered BPs in all four treated operon mutant cells (Fig. S1A, S2A, S3A, S4A). In the category of CC, cytosol, and cytoplasm, membrane and plasma membrane, integral component of membrane and plasma membrane, large and small ribosomal subunits, outer cell membrane, periplasmic space, pore complex, proton-transporting ATP synthase complex, ATP-binding cassette transporter complex, plasma membrane respiratory chain complex I or NADH dehydrogenase complex were obtained as significantly altered CCs in all treated mutant cells (Fig. S1B S2B, S3B, S4B). Whereas the common MFs observed in all treated mutant cells includes, ATP and NAD binding, DNA and RNA binding, structural constituent of ribosome, metal ion binding, magnesium, and zinc ion binding, ATPase activity, tRNA and rRNA binding, 4 iron-4 sulfur cluster binding, electron transfer activity, proton-transporting ATP synthase activity, and oxidoreductase activity (Fig. S1C, S2C, S3C, S4C). This analysis showed that the influence of hydrogenases on the persistence in *E. coli* is mediated by multiple factors and phenomena.

Discussion And Conclusion

The increased cellular viabilities of the antibiotic-treated cells of hydrogenase (large subunit gene and operon) mutants, revealed the influence of hydrogenases on persistence (Fig. 1A and 1B). Comparable lower viabilities of operon mutants than the single gene mutants pointed a more deleterious nature of operon deletion, as suggested by our previous studies on hydrogen metabolism (Shekhar et al. 2021). Hyd-2 and Hyd-3 found a relatively significant in bacterial survival against the antibiotic. However, hydrogenases were never extensively studied for their effects on drug metabolism; the uptake-hydrogenases were reported as showing a significant expression in some bacteria (Zbell et al. 2008). Our previous studies demonstrated that all the four hydrogenases of *E. coli* have uptake activity (Shekhar et al. 2021), which supports the enhanced viabilities of the mutants by influencing antibiotic metabolizing activity. Moreover, purified Hyd-1 of *Clostridium pasteurianum* was found able to reduce several 2-, 4- and 5-nitroimidazole compounds via an electron carrier-coupled mechanism indicating the influential role of hydrogenases in drug metabolism (Church et al. 1990).

hyb operon mutant showed the least growth differences when the cells were grown in the presence and absence of antibiotic. Since the persister level increases in the course of growth (Keren et al. 2004; Lewis

2019), *hyb* mutant demonstrated high feasibility of persistence as indicated by its high cellular viability (Fig. 1B). Hydrogenases were mostly studied and reported to be maximally expressed under anaerobic conditions (Vardar-Schara et al. 2008; Trchounian et al. 2012). The results till now from the operon mutants supposed to be conceivable since dissolved oxygen level was found near to zero at their mid-exponential phase (at the point of antibiotic addition to the culture) and zero at the time of treated cells collection from the cultures (3 h later of antibiotic acquisition) (Fig. 2B), therefore, the cultural conditions in which mutant cells were growing could be assigned as oxygen deprived or micro-aerobic (Shan et al. 2012). Additionally, since the persister population gets killed overtime at high levels of oxygen, and their survival requires a drop in DO (Grant et al. 2012), the micro-aerobic conditions appear feasible for the growth of persisters, in this study. Moreover, the elevated hydrogenase expression in the antibiotic-treated cells of the mutants (specifically Hyd-1, 2, and 3), demonstrated their influential role in bacterial persistence (Fig. 3).

In general, the central metabolism of the cell yields metabolites, ATP, and reduced cofactors (NADH, $FADH_2$) (Wilmaerts et al. 2019). The electron transport chain (ETC) consists of NADH dehydrogenases, and terminal oxidases and is recognized as strongly branched, which allows the cells to respond to changing environments (Borisov et al. 2011; Efremov et al. 2012). In aerobic conditions, ubiquinone accepts electrons from NADH dehydrogenase I and transports them to one of the terminal oxidases (Wilmaerts et al. 2019; Efremov et al. 2012). In this, protons are transported across the membrane, creating an electrochemical proton gradient, which drives ATP synthesis (Unden et al. 1997). Since the formation of persister cells is inversely correlated with metabolic activity and energy production (Lewis 2019), and ATP is recognized as a general cause of tolerance since most bactericidal antibiotics kill by corrupting active, energy-dependent targets (Shan et al. 2017). In hydrogenase operon mutants, ATP levels in all the antibiotic-treated cells were found variably decreased as compared to untreated cells that were grown under similar conditions (Fig. 4) indicating an influential role of hydrogenases in persister formation (Lewis 2019; Shan et al. 2017). Hyd-1 and Hyd-2 activity demonstrated to generate a transmembrane electrochemical gradient that transduced for ATP synthesis; similarly, Hyd-3 and Hyd-4 are also supposed to contribute to bacterial energy metabolism (Sargent 2016). Since *hyb* operon mutant showed relatively more percentage decreased in intracellular ATP, a more influential role of Hyd-2 could be considered in persistence. The hydrogenases affect the persistence due to low ATP might be the most straightforward interpretation of these results, indicating an influence on ETC and thereby on the membrane potential by hydrogenase operon deletions that affect the ATP synthesis and lead to antibiotic tolerance by persisters (Lewis 2019).

As mentioned above, the catabolism generates NADH, which is then oxidized by enzymes in the ETC and contributes to PMF. The elevated PMF facilitates the uptake of bactericidal antibiotics and the killing of persisters (Allison et al. 2011; Kohanski et al. 2007). At the exponential phase, persisters were found characteristically as a least redox-active subpopulation, indicating low metabolic activity is the key to the survival of persister cells (Wood et al. 2013; Mehmet et al. 2015). A relatively high and low fold change decrease in NAD/NADH ratio shown by *hyc* and *hyb* mutants respectively (Fig. 5) may indicate their

appreciable role in metabolizing NADH under the influence of antibiotic and in persistence. However, this high fold change decrease seems to be influenced by respiratory NADH dehydrogenase Complex I, since based on the sequence identity, most of its components have equivalents in Hyd-3 (Efremov et al. 2012; Marreiros et al. 2013). Although Hyd-4 is homologically related to Hyd-3 and predicted to be similar to Complex I, *hyf* operon reported not normally to be transcribed, and its detection and redox measurement are therefore challenging (Self et al. 2004; Skibinski et al. 2002). Persister survival has been attributed to the inhibition of essential cell functions during antibiotic stress, therefore; metabolism plays a critical role in this process (Amato et al. 2014; Liu et al. 2020; Cabral et al. 2018). Amino acid biosynthesis and degradation (Liu et al. 2020), carbohydrate biosynthesis and degradation (Agamennone et al. 2019), cell wall biogenesis (Costerton et al. 1975), energy metabolism (Shan et al. 2017; Cabral et al. 2018; Mohiuddin et al. 2020; Shan et al. 2017), glycolysis (Murima et al. 2014), lipid metabolism (Cañas-Duarte et al. 2020), metabolic intermediate biosynthesis (Murima et al. 2014), oxidative phosphorylation (Amato et al. 2014; Mohiuddin et al. 2020), and TCA cycle (Wang et al. 2018), are reported crucially involved in persistence and found to be contributory factors in antibiotic-treated cells of all four hydrogenase operon mutants (Fig. 6).

As reported by Kohanski et al. (2010), in the primary drug-target interaction, NADH-coupled electron transport is a key upregulated pathway that induces a surge in NADH consumption upon exposure to bactericidal antibiotics. This catabolic depletion of NADH likely induces a burst in superoxide (O^{2-}) generation via ETC. These O^{2-} damages Fe-S clusters and facilitate the formation of hydroxyl (•OH) radicals via the Fenton reaction. These •OH radicals contribute to cell death through cellular damages. The electrons are transferred to ETC via the Fe-S clusters harbored in the subunit proteins of hydrogenases, therefore considered as redox-sensitive proteins to implicate in the mechanism for antibiotic-induced cell death or persistence (Stiebritz et al. 2012). Since ROS is identified as a critical antibiotic-induced cellular stress, tolerance to antibiotics is the ability of the cell to defend itself against it (Kohanski et al. 2010). Contrary to this, according to a few reports, ROS can provide a protective effect against antibiotics by inducing persistence (Dwyer, 2014; Brynildsen, 2013). A relative decrease in ROS levels in antibiotic-treated mutant cells in comparison with PS may indicate their ROS scavenging activity (Fig. 7), where *hyb* mutant found to be able in ROS detoxification and persistence since bacterial survival against antibiotics is also reported to be mediated by such activity (Grant et al. 2012; Lewis 2019).

As previously identified crucial in persistence, the translation (Cho et al. 2015), large ribosomal subunit (Maisonneuve et al. 2011), cellular response to DNA damage stimulus (Mok et al. 2018), carbohydrate metabolic process (Agamennone et al. 2019), protein folding and transport (Scheuplein et al. 2020; May et al. 2018; Holland 2004), cell division and cycle (Aakre et al. 2012; Sass et al. 2013), response to antibiotic (Lewis 2019), TCA cycle (Wang et al. 2018), and phosphoenol pyruvate-dependent sugar phosphotransferase system (Postma et al. 1989) were also found most commonly altered biological processes in all four treated operon mutants (Fig. S1A, S2A, S3A, S4A). Similarly, cytosol, and cytoplasm (Reyes-Fernández et al. 2020), membrane and plasma membrane (May et al. 2018), integral component of membrane and plasma membrane (May et al. 2018), large and small ribosomal subunits (Wood et al.

2019; Maisonneuve et al. 2011; Romilly et al. 2014), cell outer membrane (May et al. 2018), periplasmic space (Costerton et al. 1975), pore complex (Brito et al. 2019), proton-transporting ATP synthase complex (Shan et al. 2017), ATP-binding cassette transporter complex (Lewis 2012), plasma membrane respiratory chain complex I or NADH dehydrogenase complex, cytochrome complex (Allison et al. 2011), as identified key cellular components were also obtained altered in all treated mutant cells (Fig. S1B, S2B, S3B, S4B). Finally, in the same way, the observed key molecular functions reported crucial in persistence such as ATP and NAD binding (Lewis 2012; Pu et al. 2019; Mohiuddin et al. 2020), DNA and RNA binding (Zeinert et al. 2018; Mohiuddin et al. 2020; Maisonneuve et al. 2011; Romilly et al. 2014), structural constituent of ribosome (Wood et al. 2019; Cho et al. 2015), metal ion binding (Falcón García et al. 2020), magnesium and zinc ion binding (Xu et al. 2020), ATPase activity (Shan et al. 2017), tRNA and rRNA binding (Romilly et al. 2014), 4 iron-4 sulfur cluster binding (Kohanski et al. 2010), electron transfer activity (Allison et al. 2011; Tuchscherr et al. 2020), proton-transporting ATP synthase activity (Mohiuddin et al. 2020), and oxidoreductase activity (Amato et al. 2014; Mohiuddin et al. 2020) were also found notably influenced in all antibiotic-treated mutant cells (Fig. S1C, S2C, S3C, S4C). These results demonstrate the influential roles of hydrogenases on persistence in *E. coli* (Table S1-S5).

In conclusion, hydrogenases (specifically Hyd-2 and Hyd-3) were found to have influential roles in bacterial persistence via their effects on energy (ATP), metabolism (NADH), and ROS generation. Moreover, hydrogenases were also demonstrated to influence transcriptome broadly in persistence. This study also showed that the hydrogenases may have a potential ability to influence membrane physiology and thereby cellular metabolism.

Declarations

Funding and acknowledgments

The authors thank the Inamori Foundation, Japan to support this study.

Conflict of interest/Competing interests

The authors declare that they have no conflict of interest.

Author Contributions

CS and TM designed the study. Mostly the experiments were performed by CS. TK performed a cell viability assay. CS did transcriptomic data analysis and wrote the manuscript. TKW helped in providing assay protocol and valuable research suggestions. All authors read and approved the manuscript.

Ethics approval

This article does not contain any studies with human participants or animals performed by any of the authors.

Data availability

The transcriptomic raw sequence data can be accessed through the NCBI under the SRA accession number PRJNA671558.

References

1. Aakre CD, Laub MT (2012) Asymmetric cell division: a persistent issue? Dev Cell 22:235-236. doi: 10.1016/j.devcel.2012.01.016.
2. Agamennone V, Le NG, van Straalen NM, Brouwer A, Roelofs D (2019) Antimicrobial activity and carbohydrate metabolism in the bacterial metagenome of the soil-living invertebrate *Folsomia candida*. Sci Rep 9:7308. doi: 10.1038/s41598-019-43828-w.
3. Allison KR, Brynildsen MP, Collins JJ (2011) Metabolite-enabled eradication of bacterial persisters by aminoglycosides. Nature 473:216–220. doi: 10.1038/nature10069.
4. Amato SM, Fazen CH, Henry TC, Mok WW, Orman MA, Sandvik EL et al (2014) The role of metabolism in bacterial persistence. Front Microbiol 5:70. doi: 10.3389/fmicb.2014.00070.
5. Andrews S (2010) Fastqc A Quality Control Tool For High Throughput Sequence Data. Available from http://www.bioinformatics.babraham.ac.uk/projects/fastqc [accessed August 27, 2020].
6. Andrews SC, Berks BC, McClay J, Ambler A, Quail MA, Golby P et al (1997) A 12-cistron *Escherichia coli* operon (*hyf*) encoding a putative proton-translocating formate hydrogenlyase system. Microbiology 143:3633-3647. doi: 10.1099/00221287-143-11-3633.
7. Batista AP, Marreiros BC, Pereira MM (2013) The antiporter-like subunit constituent of the universal adaptor of complex I, group 4 membrane-bound [NiFe]- hydrogenases and related complexes. Biol Chem 394:659–666. doi: 10.1515/hsz-2012-0342.
8. Benoit SL, Schmalstig AA, Glushka J, Maier SE, Edison AE, Maier RJ (2019) Nickel chelation therapy as an approach to combat multi-drug resistant enteric pathogens. Sci Rep 9:13851. doi: 10.1038/s41598-019-50027-0.
9. Böhm R, Sauter M, Böck A (1990) Nucleotide sequence and expression of an operon in *Escherichia coli* coding for formate hydrogenlyase components. Mol Microbiol 4:231–243. doi: 10.1111/j.1365-2958.1990.tb00590.x.
10. Borisov VB, Gennis RB, Hemp J, Verkhovsky MI (2011) The cytochrome bd respiratory oxygen reductases. Biochim Biophys Acta 1807:1398–1413. doi: 10.1016/j.bbabio.2011.06.016.
11. Brito C, Cabanes D, Sarmento Mesquita F, Sousa S (2019) Mechanisms protecting host cells against bacterial pore-forming toxins. Cell. Mol Life Sci 76:1319–1339. doi: 10.1007/s00018-018-2992-8.
12. Brondsted L, Atlung T (1996) Effect of growth conditions on expression of the acid phosphatase (cyx-appA) operon and the appY gene, which encodes a transcriptional activator of *Escherichia coli*. J Bacteriol 178:1556–1564. doi: 10.1128/jb.178.6.1556-1564.1996.

13. Brynildsen MP, Winkler JA, Spina CS, MacDonald IC, Collins JJ (2013) Potentiating antibacterial activity by predictably enhancing endogenous microbial ROS production. Nat Biotechnol 31:160–165. doi: 10.1038/nbt.2458.
14. Cabral DJ, Wurster JI, Belenky P (2018) Antibiotic Persistence as a Metabolic Adaptation: Stress, Metabolism, the Host, and New Directions. Pharmaceuticals (Basel) 11:14. doi: 10.3390/ph11010014.
15. Cañas-Duarte S, Perez-Lopez M, Herrfurth C, Sun L, Contreras L, Feussner I et al (2020) An integrative approach points to membrane composition as a key factor in *E. coli* persistence. bioRxiv 2020.08.28.271171. doi: 10.1101/2020.08.28.271171.
16. Cho J, Rogers J, Kearns M, Leslie M, Hartson SD, Wilson KS (2015) *Escherichia coli* persister cells suppress translation by selectively disassembling and degrading their ribosomes. Mol Microbiol 95:352-364. doi: 10.1111/mmi.12884.
17. Chowdhury N, Kwan BW, Wood TK (2016) Persistence Increases in the Absence of the Alarmone Guanosine Tetraphosphate by Reducing Cell Growth. Sci Rep 6:20519. doi: 10.1038/srep20519.
18. Church DL, Rabin HR, Laishley EJ (1990) Reduction of 2- , 4- and 5-nitroimidazole drugs by hydrogenase 1 in *Clostridium pasteurianum*. J Antimicrob Chemother 25:15-23. doi: 10.1093/jac/25.1.15.
19. Cordero PRF, Grinter R, Hards K, Cryle MJ, Warr CG, Cook GM et al (2019) Two uptake hydrogenases differentially interact with the aerobic respiratory chain during mycobacterial growth and persistence. J Biol Chem 294:18980-18991. doi: 10.1074/jbc.RA119.011076.
20. Costerton JW, Cheng KJ (1975) The role of the bacterial cell envelope in antibiotic resistance. J Antimicrob Chemother 1:363–377. doi: 10.1093/jac/1.4.363.
21. Datsenko KA, Wanner BL (2000) One-step inactivation of chromosomal genes in *Escherichia coli* K-12 using PCR products. Proc Natl Acad Sci USA 97:6640-6645. doi: 10.1073/pnas.120163297.
22. Dwyer DJ, Belenky PA, Yang JH, MacDonald IC, Martell JD, Takahashi N et al (2014) Antibiotics induce redox-related physiological alterations as part of their lethality. Proc Natl Acad Sci USA 111:E2100–2109. doi: 10.1073/pnas.1401876111.
23. Efremov RG, Sazanov LA (2012) The coupling mechanism of respiratory complex I—A structural and evolutionary perspective. Biochim Biophys Acta 1817:1785–1795. doi: 10.1016/j.bbabio.2012.02.015.
24. Grant SS, Kaufmann BB, Chand NS, Haseley N, Hung DT (2012) Eradication of bacterial persisters with antibiotic-generated hydroxyl radicals. Proc Natl Acad Sci USA 109:2147–12152. doi: 10.1073/pnas.1203735109.
25. Holland IB (2004) Translocation of bacterial proteins--an overview. Biochim Biophys Acta 1694:5-16. doi: 10.1016/j.bbamcr.2004.02.007.
26. Hong SH, Wang X, O'Connor HF, Benedik MJ, Wood TK (2012) Bacterial persistence increases as environmental fitness decreases. Microb Biotechnol 5:509–522. doi: 10.1111/j.1751-7915.2011.00327.x.

27. Kanehisa M, Goto S (2000) KEGG: kyoto encyclopedia of genes and genomes. Nucleic Acids Res 28:27-30. doi: 10.1093/nar/28.1.27.
28. Keren I, Kaldalu N, Spoering A, Wang Y, Lewis K (2004) Persister cells and tolerance to antimicrobials. FEMS Microbiol Lett 230:13–18. doi: 10.1016/S0378-1097(03)00856-5.
29. Kohanski MA, Dwyer DJ, Hayete B, Lawrence CA, Collins JJ (2007) A common Mechanism of Cellular Death Induced by Bactericidal Antibiotics. Cell 130:797–810. doi: 10.1016/j.cell.2007.06.049.
30. Lewis K (2019) Persister Cells and Infectious Disease. Springer International Publishing. doi: 10.1007/978-3-030-25241-0.
31. Lewis VG, Ween MP, McDevitt CA (2012) The role of ATP-binding cassette transporters in bacterial pathogenicity. Protoplasma 249:919-942. doi: 10.1007/s00709-011-0360-8.
32. Liu Q, Chen N, Chen H, Huang Y (2020) RNA-Seq analysis of differentially expressed genes of *Staphylococcus epidermidis* isolated from postoperative endophthalmitis and the healthy conjunctiva. Sci Rep 10:14234. doi: 10.1038/s41598-020-71050-6.
33. Liu Y, Yang K, Zhang H, Jia Y, Wang Z (2020) Combating Antibiotic Tolerance Through Activating Bacterial Metabolism. Front Microbiol 11:577564. doi: 10.3389/fmicb.2020.577564.
34. Maeda T, Sanchez-Torres V, Wood TK (2007) Enhanced hydrogen production from glucose by metabolically engineered *Escherichia coli*. Appl Microbiol Biotechnol 77:879-890. doi: 10.1007/s00253-007-1217-0.
35. Maeda T, Tran KT, Yamasaki R, Wood TK (2018) Current state and perspectives in hydrogen production by *Escherichia coli*: roles of hydrogenases in glucose or glycerol metabolism. Appl Microbiol Biotechnol 102:2041–2050. doi: 10.1007/s00253-018-8752-8.
36. Maier L, Barthel M, Stecher B, Maier RJ, Gunn JS, Hardt WD (2014) *Salmonella Typhimurium* strain ATCC14028 requires H_2-hydrogenases for growth in the gut, but not at systemic sites. PloS One 9:e110187. doi: 10.1371/journal.pone.0110187.
37. Maisonneuve E, Gerdes K (2014) Molecular Mechanisms underlying Bacterial Persisters. Cell 157:539-548. doi: 10.1016/j.cell.2014.02.050.
38. Maisonneuve E, Shakespeare LJ, Jørgensen MG, Gerdes K (2011) Bacterial persistence by RNA endonucleases. Proc Natl Acad Sci USA 108:13206-13211. doi: 10.1073/pnas.1100186108.
39. Marreiros BC, Batista AP, Duarte AM, Pereira MM (2013) A missing link between complex I and group 4 membrane-bound [NiFe] hydrogenases. Biochim Biophys Acta 1827:198–209. doi: 10.1016/j.bbabio.2012.09.012.
40. Martin M (2011) Cutadapt removes adapter sequences from high-throughput sequencing reads. EMBnet journal 17:10-12. doi: 10.14806/ej.17.1.200.
41. May KL, Grabowicz M (2018) The bacterial outer membrane is an evolving antibiotic barrier. Proc Natl Acad Sci USA 115:8852-8854. doi: 10.1073/pnas.1812779115.
42. McClure R, Balasubramanian D, Sun Y, Bobrovskyy M, Sumby P, Genco CA et al (2013) Computational analysis of bacterial RNA-Seq data. Nucleic Acids Res 41:e140. doi:

10.1093/nar/gkt444.

43. Mehmet AO, Brynildsen MP (2015) Inhibition of stationary phase respiration impairs persister formation in *E. coli*. Nat Commun 6:7983. doi: 10.1038/ncomms8983.
44. Mohiuddin SG, Hoang T, Saba A, Karki P, Orman MA (2020) Identifying Metabolic Inhibitors to Reduce Bacterial Persistence. Front Microbiol 11:472. doi: 10.3389/fmicb.2020.00472.
45. Mok WWK, Brynildsen MP (2018) Timing of DNA damage responses impacts persistence to fluoroquinolones. Proc Natl Acad Sci USA 115:E6301-E6309. doi: 10.1073/pnas.1804218115.
46. Murima P, McKinney JD, Pethe K (2014) Targeting bacterial central metabolism for drug development. Chem Biol 21:1423-1432. doi: 10.1016/j.chembiol.2014.08.020.
47. Mustapha NA, Hu A, Yu CP, Sharuddin SS, Ramli N, Shirai Y et al (2018) Seeking key microorganisms for enhancing methane production in anaerobic digestion of waste sewage sludge. Appl Microbiol Biotechnol 102:5323-5334. doi: 10.1007/s00253-018-9003-8.
48. Nie W, Tang H, Fang Z, Chen J, Chen H, Xiu Q (2012) Hydrogenase: the next antibiotic target? Clin Sci 122:575–580. doi: 10.1042/CS20110396.
49. Ohsawa I, Ishikawa M, Takahashi K, Watanabe M, Nishimaki K, Yamagata K et al (2007) Hydrogen acts as a therapeutic antioxidant by selectively reducing cytotoxic oxygen radicals. Nat Med 13:688–694. doi: 10.1038/nm1577.
50. Olson JW, Maier RJ (2002) Molecular hydrogen as an energy source for *Helicobacter pylori*. Science 298:1788–1790. doi: 10.1126/science.1077123.
51. Pecher A, Zinoni F, Jatisatienr C, Wirth R, Hennecke H, Böck A (1983) On the Redox Control of Synthesis of Anaerobically Induced Enzymes in Enterobacteriaceae. Arch Microbiol 136:131-136. doi: 10.1007/BF00404787.
52. Pfaffl MW (2001) A new mathematical model for relative quantification in real-time RT–PCR. Nucleic Acids Res 29:45e. doi: 10.1093/nar/29.9.e45.
53. Pinske C, Jaroschinsky M, Linek S, Kelly CL, Sargent F, Sawers RG (2015) Physiology and bioenergetics of [NiFe]-hydrogenase 2-catalyzed H_2-consuming and H_2-producing reactions in *Escherichia coli*. J Bacteriol 197:296–306. doi: 10.1128/JB.02335-14.
54. Postma PW, Broekhuizen CP, Geerse RH (1989) The role of the PEP: carbohydrate phosphotransferase system in the regulation of bacterial metabolism. FEMS Microbiol Rev 5:69–80. doi: 10.1016/0168-6445(89)90010-7.
55. Pu Y, Li Y, Jin X, Tian T, Ma Q, Zhao Z et al (2019) ATP-Dependent Dynamic Protein Aggregation Regulates Bacterial Dormancy Depth Critical for Antibiotic Tolerance. Mol Cell 73:143-156.e4. doi: 10.1016/j.molcel.2018.10.022.
56. Reyes-Fernández EZ, Schuldiner S (2020) Acidification of Cytoplasm in *Escherichia coli* Provides a Strategy to Cope with Stress and Facilitates Development of Antibiotic Resistance. Sci Rep 10:9954. doi: 10.1038/s41598-020-66890-1.

57. Richard DJ, Sawers G, Sargent F, McWalter L, Boxer DH (1999) Transcriptional regulation in response to oxygen and nitrate of the operons encoding the [NiFe] hydrogenases 1 and 2 of *Escherichia coli*. Microbiology 145:2903-2912. doi: 10.1099/00221287-145-10-2903.

58. Robinson MD, McCarthy DJ, Smyth GK (2010) edgeR: a Bioconductor package for differential expression analysis of digital gene expression data. Bioinformatics 26:139-140. doi: 10.1093/bioinformatics/btp616.

59. Romilly C, Lays C, Tomasini A, Caldelari I, Benito Y, Hammann P et al (2014) A non-coding RNA promotes bacterial persistence and decreases virulence by regulating a regulator in *Staphylococcus aureus*. PLoS Pathog 10:e1003979. doi: 10.1371/journal.ppat.1003979.

60. Sanchez-Torres V, Yusoff MZ, Nakano C, Maeda T, Ogawa HI, Wood TK (2013) Influence of *Escherichia coli* hydrogenases on hydrogen fermentation from glycerol. Int J Hydrog Energy 38: 3905-3912. doi: 10.1016/j.ijhydene.2013.01.031.

61. Sargent F (2016) The Model [NiFe]-Hydrogenases of *Escherichia coli*. Adv Microb Physiol 68:433-507. doi: 10.1016/bs.ampbs.2016.02.008.

62. Sass P, Brötz-Oesterhelt H (2013) Bacterial cell division as a target for new antibiotics. Curr Opin Microbiol 16:522-530. doi: 10.1016/j.mib.2013.07.006.

63. Scheuplein NJ, Bzdyl NM, Kibble EA, Lohr T, Holzgrabe U, Sarkar-Tyson M (2020) Targeting Protein Folding: A Novel Approach for the Treatment of Pathogenic Bacteria. J Med Chem 63:13355-13388. doi: 10.1021/acs.jmedchem.0c00911.

64. Self WT, Hasona A, Shanmugam KT (2004) Expression and regulation of a silent operon, hyf, coding for hydrogenase 4 isoenzyme in *Escherichia coli*. J Bacteriol 186:580–587. doi: 10.1128/jb.186.2.580-587.2004.

65. Shan Y, Gandt AB, Rowe SE, Deisinger JP, Conlon BP, Lewis K (2017) ATP dependent persister formation in *Escherichia coli*. mBio 8:e02267-16. doi:10.1128/mBio.02267-16.

66. Shan Y, Lai Y, Yan A (2012) Metabolic reprogramming under microaerobic and anaerobic conditions in bacteria. Subcell Biochem 64:159-79. doi: 10.1007/978-94-007-5055-5_8.

67. Shekhar C, Kai T, Garcia-Contreras R, Sanchez-Torres V, Maeda T (2021) Evaluation of Hydrogen Metabolism by *Escherichia coli* Strains Possessing Only the Single Hydrogenase in the Genome. Int J Hydrog Energy 46:1728-1739. doi: 10.1016/j.ijhydene.2020.10.070

68. Skibinski DA, Golby P, Chang YS, Sargent F, Hoffman R, Harper R et al (2002) Regulation of the hydrogenase-4 operon of *Escherichia coli* by the sigma (54)-dependent transcriptional activators FhlA and HyfR. J Bacteriol 184:6642–6653. doi: 10.1128/jb.184.23.6642-6653.2002.

69. Stiebritz MT, Reiher M (2012) Hydrogenases and oxygen. Chem Sci 3:1739-1751. doi: 10.1039/C2SC01112C.

70. Trchounian K, Poladyan A, Vassilian A, Trchounian A (2012) Multiple and reversible hydrogenases for hydrogen production by *Escherichia coli*: dependence on fermentation substrate, pH and the F0F1-ATPase. Crit Rev Biochem Mol Biol 47:236–249. doi: 10.3109/10409238.2012.655375.

71. Tuchscherr L, Löffler B, Proctor RA (2020) Persistence of Staphylococcus aureus: Multiple Metabolic Pathways Impact the Expression of Virulence Factors in Small-Colony Variants (SCVs). Front Microbiol 11:1028. doi: 10.3389/fmicb.2020.01028.
72. Unden G, Bongaerts J (1997) Alternative respiratory pathways of *Escherichia coli*: Energetics and transcriptional regulation in response to electron acceptors. Biochim Biophys Acta 1320:217–234. doi: 10.1016/S0005-2728(97)00034-0.
73. Vardar-Schara G, Maeda T, Wood TK (2008) Metabolically engineered bacteria for producing hydrogen via fermentation. Microb Biotechnol 1:107–25. doi: 10.1111/j.1751-7915.2007.00009.x.
74. Wang T, Meouche IE, Dunlop MJ (2017) Bacterial persistence induced by salicylate via reactive oxygen species. Sci Rep 7:43839. doi: 10.1038/srep43839.
75. Wang Y, Bojer MS, George SE, Wang Z, Jensen PR, Wolz C et al (2018) Inactivation of TCA cycle enhances *Staphylococcus aureus* persister cell formation in stationary phase. Sci Rep 8:10849. doi: 10.1038/s41598-018-29123-0.
76. Wilmaerts D, Windels EM, Verstraeten N, Michiels J (2019) General Mechanisms Leading to Persister Formation and Awakening. Trends Genet 35:401-411. doi: 10.1016/j.tig.2019.03.007.
77. Wood TK (2016) Combatting bacterial persister cells. Biotechnol Bioeng 113:476-483. doi: 10.1002/bit.25721.
78. Wood TK, Knabel SJ, Kwan BK (2013) Bacterial Persister Cell Formation and Dormancy. Appl Environ Microbiol 79:7116–7121. doi: 10.1128/AEM.02636-13.
79. Wood TK, Song S, Yamasaki R (2019) Ribosome dependence of persister cell formation and resuscitation. J Microbiol 57:213-219. doi: 10.1007/s12275-019-8629-2.
80. Xu T, Wang X, Meng L, Zhu M, Wu J, Xu Y et al (2020) Magnesium Links Starvation-Mediated Antibiotic Persistence to ATP. mSphere 5:e00862-19. doi: 10.1128/mSphere.00862-19.
81. Young MD, Wakefield MJ, Smyth GK, Oshlack A (2010) Gene ontology analysis for RNA-seq: accounting for selection bias. Genome Biol 11:R14. doi: 10.1186/gb-2010-11-2-r14.
82. Zbell AZ, Maier SE, Maier RJ (2008) *Salmonella enterica* Serovar Typhimurium NiFe Uptake-Type Hydrogenases Are Differentially Expressed in Vivo. Infect Immun 76:4445–4454. doi: 10.1128/IAI.00741-08.
83. Zeinert RD, Liu J, Yang Q, Du Y, Haynes CM, Chien P (2018) A legacy role for DNA binding of Lon protects against genotoxic stress. bioRxiv 317677. doi: 10.1101/317677.

Tables

Table 1

E. coli strains used in this study

Strains/plasmids	Genotype/relevant characteristics	Reference
E. coli BW25113	F^-Δ(*araD-araB*)567ΔlacZ4787 (::rrnB-3)λ^- *rph-1* Δ(*rhaD-rhaB*) 568 *hsdR*514; parental strain for the Keio collection	Yale Coli Genetic Stock Center
E. coli BW25113 Δ[a] *hyaA-F*[c]::[b] *kan*[d]	Hyd-1 operon deleted mutant	(Shekhar et al. 2021)
E. coli BW25113 Δ*hybO-F::kan*	Hyd-2 operon deleted mutant	(Shekhar et al. 2021)
E. coli BW25113 Δ*hycA-I::kan*	Hyd-3 operon deleted mutant	(Shekhar et al. 2021)
E. coli BW25113 Δ*hyfA-R::kan*	Hyd-4 operon deleted mutant	(Shekhar et al. 2021)
E. coli BW25113 Δ*hyaB::kan*	Hyd-1 large subunit gene deleted mutant	(Sanchez-Torres et al. 2013)
E. coli BW25113 Δ*hybC::kan*	Hyd-2 large subunit gene deleted mutant	(Sanchez-Torres et al. 2013)
E. coli BW25113 Δ*hycE::kan*	Hyd-3 large subunit gene deleted mutant	(Sanchez-Torres et al. 2013)
E. coli BW25113 Δ*hyfG::kan*	Hyd-4 large subunit gene deleted mutant	(Sanchez-Torres et al. 2013)

a and b: Δ and :: represents “deletion” and “replaced by gene,” respectively.

c: *A-F*, *O-F*, *A-I*, and *A-R* represents the “from and to” deleted segment of *hya*, *hyb*, *hyc*, and *hyf* operons, respectively.

d: *kan* denotes kanamycin resistance gene.

Table 2

List of primers used in qRT-PCR

Primer	Significance	Sequence (5'-3')	Reference
hyaB-F	Expressing large subunit gene of Hyd-1	CACGGCGGACTTCATTAACA	This study
hyaB-R		CCGTAGCTGAGAACGCATTTAT	
hybC-F	Expressing large subunit gene of Hyd-2	CAAACTGAGCGACTTTGTTGAG	This study
hybC-R		GGTAGTTCACCGCACCTTTA	
hycE-F	Expressing large subunit gene of Hyd-3	CCATTCTGCTGGAGGTAGAAC	This study
hycE-R		ACGCGGAAGAACTGCATAA	
hyfG-F	Expressing large subunit gene of Hyd-4	CTGCATATCACCTCCGATGAA	This study
hyfG-R		TGCCGCGATGGACATAAA	
rrsG-F	Housekeeping gene for expression data	TATTGCACAATGGGCGCAAG	(Sanchez-Torres et al. 2013)
rrsG-R		ACTTAACAAACCGCCTGCGT	

F and R represent forward and reverse primers, respectively.

Figures

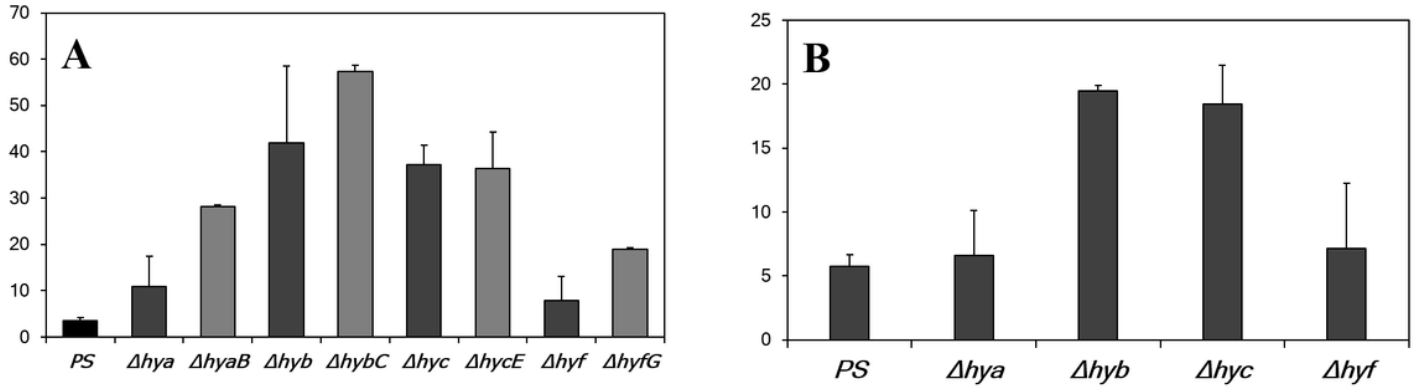

Figure 1

Enhanced cell viability of hydrogenase operon mutants after antibiotic treatment. Cellular viability of the hydrogenase large subunit gene and entire operon deleted mutants before and after antibiotic treatment under micro-aerobic (oxygen deprived) (**A**) and of the operon mutants under anaerobic conditions (**B**). Cell viability was calculated by dividing the cfu/mL obtained from the antibiotic-treated culture by the cfu/mL obtained from the initial cells. Data are the mean of three independent assays; error bars indicating stdev.

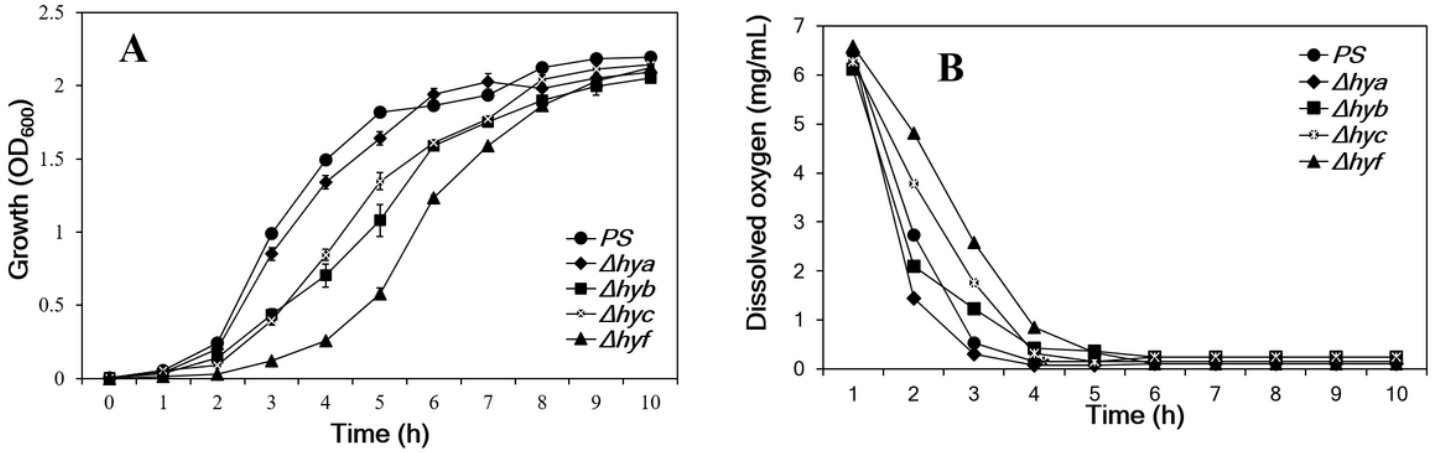

Figure 2

The influenced growth by antibiotic and the role of dissolved oxygen. **(A)** Growth curves of the operon mutants and comparison with the PS. **(B)** DO concentrations in the cultures of the strains at different time points of the persister assay. Data represent the average of two replicates. Error bars represent STDEV.

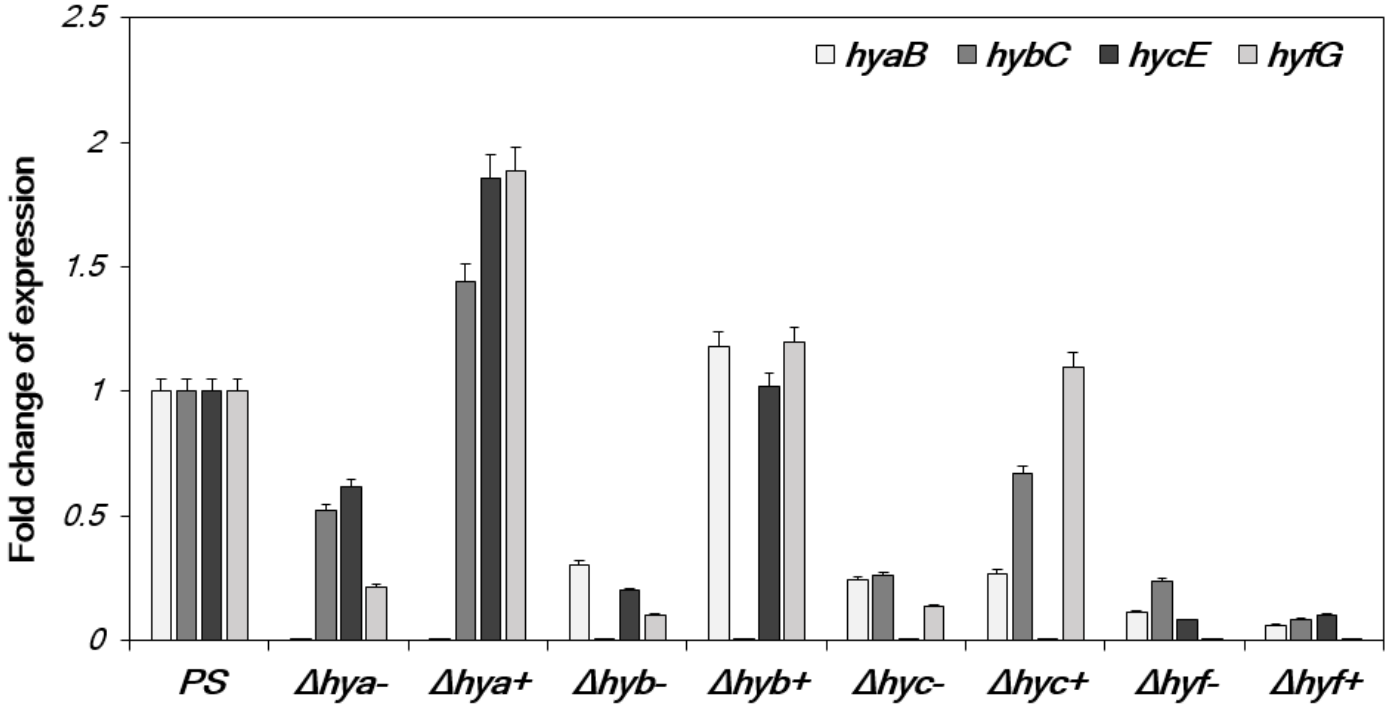

Figure 3

Elevated hydrogenase expressions in the antibiotic-treated hydrogenase mutant cells. The fold change expression levels of hydrogenases (genes encoding large subunit) in four hydrogenase operon mutants

grown in the absence (-) and presence (+) of the antibiotic (i.e., initial, and treated cells). The relative expression level was normalized with a housekeeping gene, *rrsG* (16S rRNA). The bars indicate the mean of the triplicates; the error bar indicates STDEV.

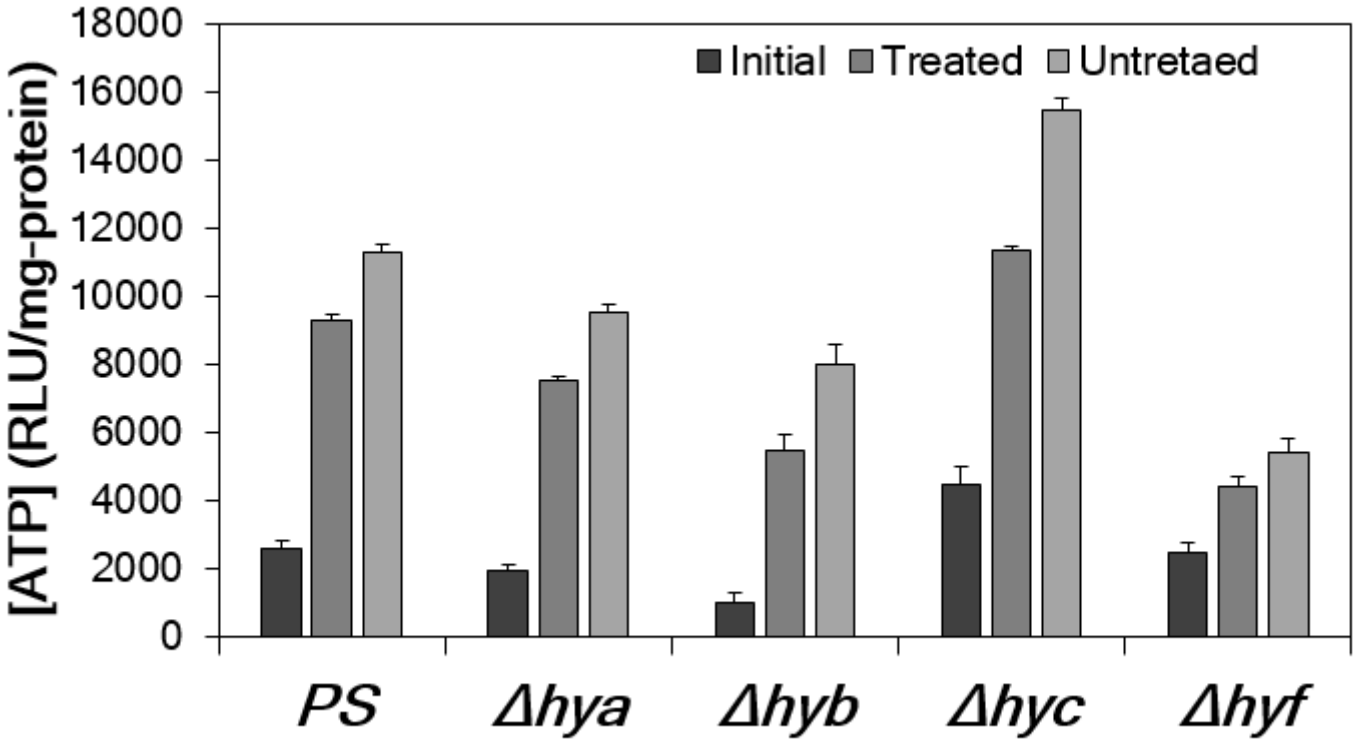

Figure 4

Reduced ATP in the antibiotic-treated mutant cells. ATP quantification from the cultures of the initial, treated, and untreated operon mutant cells, including the PS. Total protein was calculated as 0.22 mg/mL/OD_{600}. Error bars show standard deviation from quintuplets.

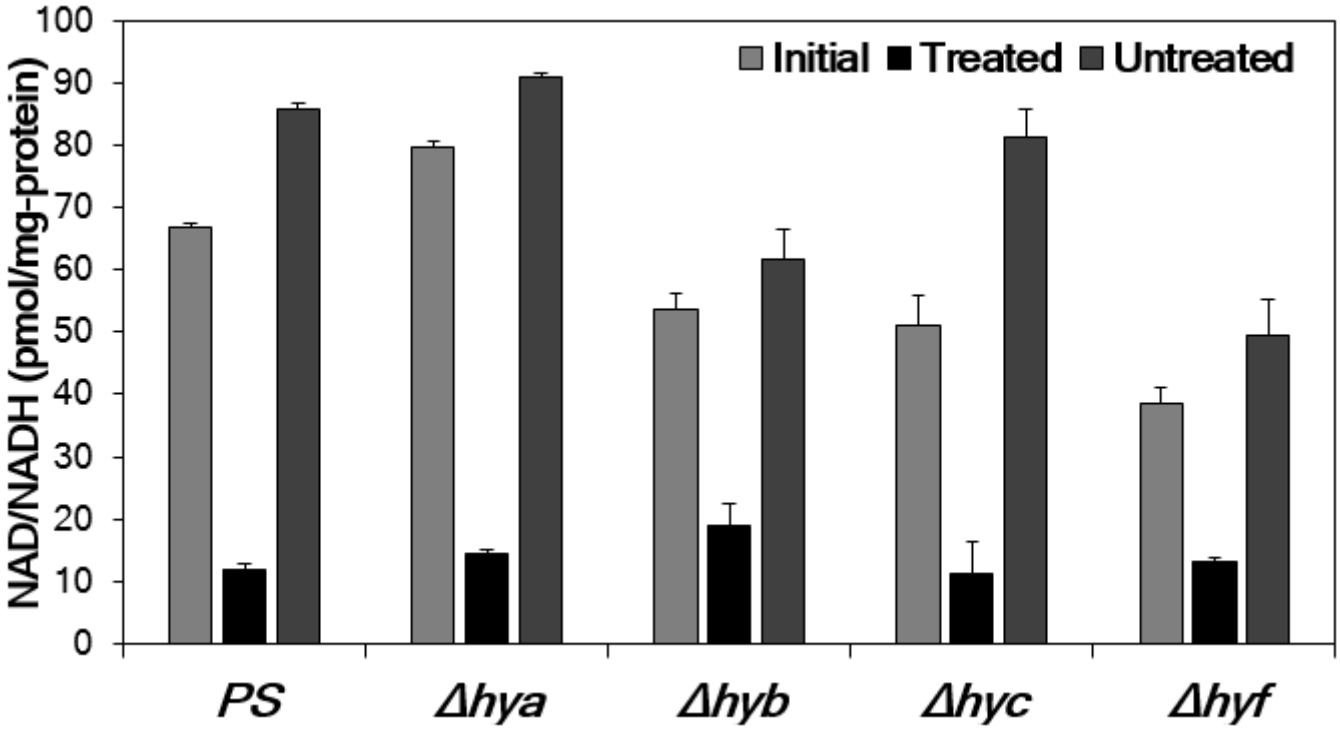

Figure 5

Decreased NAD content in the antibiotic-treated mutant cells. NAD/NADH ratio was estimated from the cultures of the initial, treated, and untreated operon mutant cells, including the PS. NAD indicates the sum of NAD^+ and NADH. Total protein was calculated as 0.22 mg/mL/OD_{600}. Error bars show standard deviation from biological triplicates.

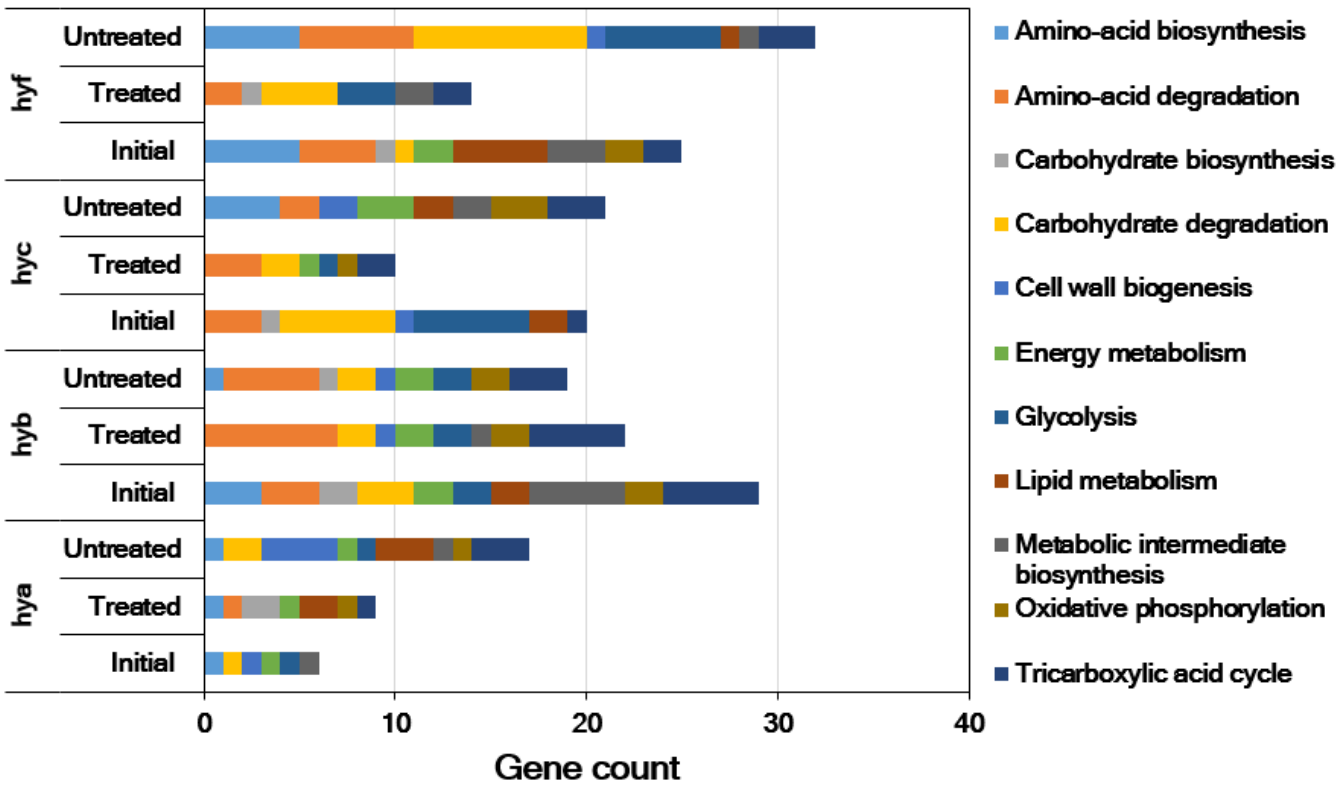

Figure 6

Antibiotic affected metabolism in the mutant cells. The key metabolic pathways in the initial, treated, and untreated mutant cells were identified by KEGG pathway enrichment analysis. The data from the mutant strains were normalized with that of the PS. A full list of all the KEGG terms is available in Table S4A-4D.

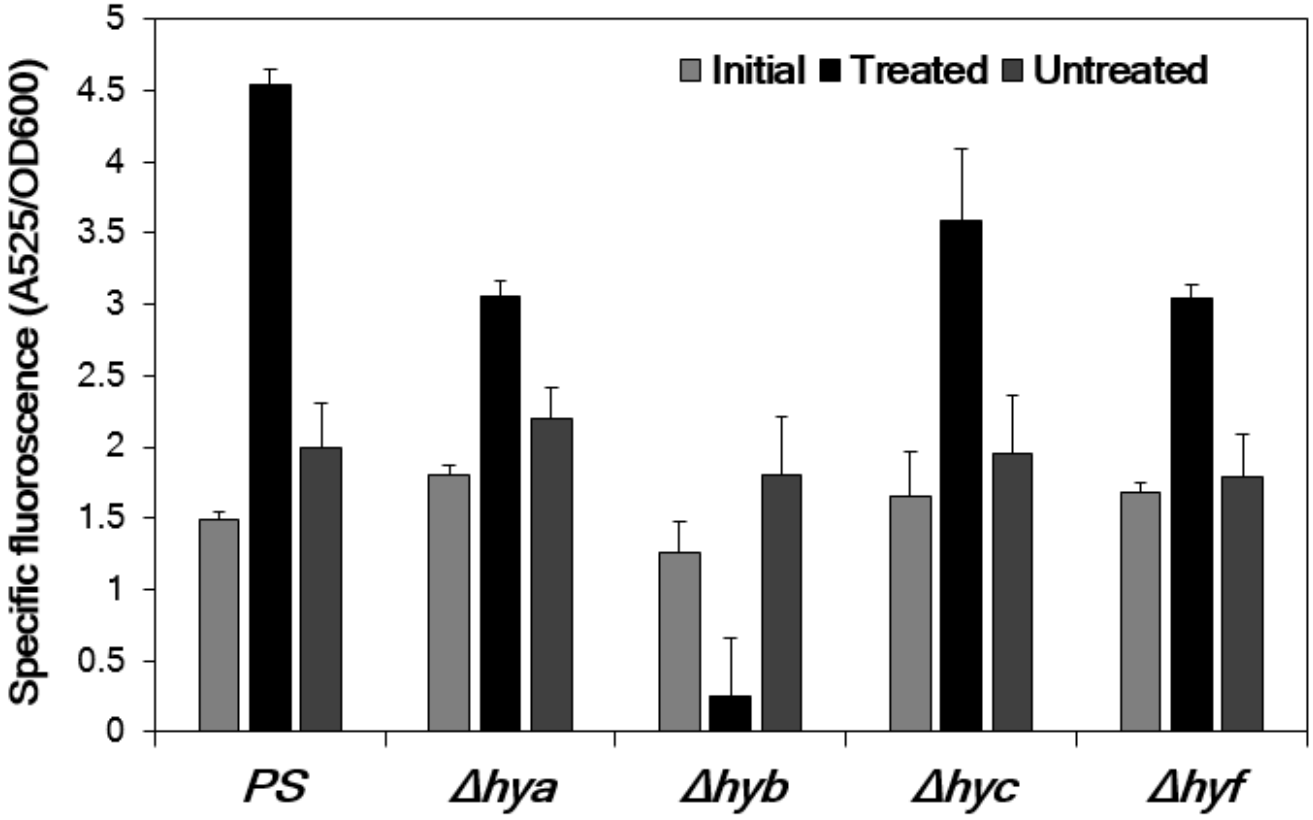

Figure 7

Altered ROS levels in antibiotic-treated mutant cells. ROS quantification from the hydrogenase operon mutant and PS cells before and after the addition of the antibiotic to the cultures. The specific fluorescence is calculated as A_{525}/OD_{600} from the cultures treated with the general ROS indicator carboxy-H_2DCFDA. Error bars show the standard deviation of the biological triplicates.

Supplementary Files

This is a list of supplementary files associated with this preprint. Click to download.

- SupplementarymaterialsIMchandra.pdf